New Journal of Physics

An Institute of Physics and Deutsche Physikalische Gesellschaft Journal

Prospects for SIMPLE 2000: a large-mass, low-background superheated droplet detector for WIMP searches

J I Collar[1,2,6], J Puibasset[1], T A Girard[3], D Limagne[1], H S Miley[4] and G Waysand[1,5]

[1] Groupe de Physique des Solides (UMR CNRS 75-88), Universités Paris 7 et 6, 75251 Paris Cedex 05, France
[2] CERN, EP Division, CH-1211 Genève 23, Switzerland
[3] Centro de Física Nuclear, Universidade de Lisboa, 1649-003 Lisboa, Portugal
[4] Pacific Northwest National Laboratory, Richland, WA 99352, USA
[5] Laboratoire Souterrain à Bas Bruit de Rustrel-Pays d'Apt, Rustrel 84400, France

[6] Corresponding author
E-mail: juan.collar@cern.ch

New Journal of Physics **2** (2000) 14.1–14.14 (http://www.njp.org/)
Received 6 March 2000; online 13 July 2000

Abstract. The Superheated Instrument for Massive Particle searches (SIMPLE 2000) will consist of an array of 8–16 large active mass ($\simeq$15 g) superheated droplet detectors (SDDs) to be installed in the new underground laboratory of Rustrel-Pays d'Apt. Several factors make the use of SDDs an attractive approach for the detection of weakly interacting massive particles (WIMPs), namely their intrinsic insensitivity to minimally ionizing particles, high fluorine content, low cost and operation at near ambient pressure and temperature. We comment here on the fabrication, calibration and already-competitive first limits from prototype SDDs for SIMPLE, as well as on the expected immediate increase in sensitivity of the programme, which aims at an exposure of $>$25 kg day during 2000. The ability of modest-mass fluorine-rich detectors to investigate regions of neutralino parameter space beyond the reach of the most ambitious cryogenic projects is pointed out.

Apfel extended the bubble chamber concept by the invention of superheated droplet detectors [1] (SDDs, also known as bubble detectors), a dispersion of small drops (radius $\simeq$10 μm) of superheated liquid in a gel or viscoelastic matrix. The SDD matrix isolates the fragile metastable system from vibrations and especially from convection currents (which are absent in gels), while the smooth liquid–liquid interfaces impede the continuous triggering on surface impurities that occurs in the walls and gaskets of even the cleanest bubble chambers. A physically sound metaphor for the gain in stability of SDDs over that of bubble chambers is the improvement that was brought about by using dynamite instead of nitroglycerine: in SDDs, the lifetime of the superheated state is extended to the point that new practical applications such as personnel and area neutron dosimetry become possible.

In the moderately superheated liquids used in SDDs, bubbles can be produced only by particles having elevated stopping powers ($\mathrm{d}E/\mathrm{d}x \geq 200$ keV $\mu\mathrm{m}^{-1}$) as is the case for low-energy nuclear recoils. This behaviour is described by Seitz's classical 'thermal spike' model [2]: for the transition to occur, a vapour nucleus or 'protobubble' of radius $>r_c$ must be created, while only the energy deposited along a distance comparable to this critical radius r_c is available for its formation. Hence, a double threshold is imposed: the requirement that the deposited energy E be larger than the thermodynamical work of formation of the critical nucleus, E_c, and that this energy be lost by the particle over a distance $O(r_c)$, i.e. a minimum stopping power. Protobubbles formed by depositions of energy not satisfying both demands simply shrink back to zero; otherwise, the transition is irreversible and the whole droplet vaporizes. Formally expressed, these two conditions become [3, 4]:

$$\begin{aligned} &E > E_c = 4\pi r_c^2 \gamma/(3\epsilon) \\ &\mathrm{d}E/\mathrm{d}x > E_c/(a r_c) \end{aligned} \tag{1}$$

where $r_c = 2\gamma/\Delta P$, $\gamma(T)$ is the surface tension, $\Delta P = P_V - P$, $P_V(T)$ is the vapour pressure of the liquid (generally an industrial refrigerant), P and T are the operating pressure and temperature, ϵ varies in the range $[0.02, 0.06]$ for various liquids [4, 5], and $a(T) \sim O(1)$ [6]. The parameter ϵ is of particular importance in the calculation of the minimum recoil energy that needs to be transferred in a neutron (or WIMP) collision for a bubble to form, given that in most cases these recoils have a sufficiently high $\mathrm{d}E/\mathrm{d}x$ to pass the second requirement. The physical meaning of ϵ is often misinterpreted by modern authors as a somewhat undefined fraction of deposited energy available for protobubble formation. The reality (which was well known during the bubble chamber era) is different: making $\epsilon = 1$, E_c as calculated in equation (1) becomes equal to the minimum (Gibbs) bubble expansion work, a gross but convenient underestimate of the actual work of bubble formation. Examining the process in detail, E_c can be recalculated as the much larger sum of the reversible works of bubble surface formation, evaporation of the liquid and expansion against P [4, 6]:

$$E_c' = 4\pi r_c^2 \left(\gamma - T\frac{\partial \gamma}{\partial T}\right) + \frac{4}{3}\pi r_c^3 \rho_v \frac{h_{fg}}{M} + \frac{4}{3}\pi r_c^3 P \tag{2}$$

where ρ_v is the saturated vapour density, h_{fg} is the latent heat of vaporization per mole and M is the molecular mass. On making

$$\epsilon = 4\pi r_c^2 \gamma/(3E_c') \tag{3}$$

equation (1) acquires a compact form but leads to the conceptual misunderstanding mentioned above. It must be emphasized that ϵ as correctly defined in equation (3) is not a free parameter: it can be accurately calculated for each refrigerant and operating condition (figure 1) and compared with experimental measurements (see below).

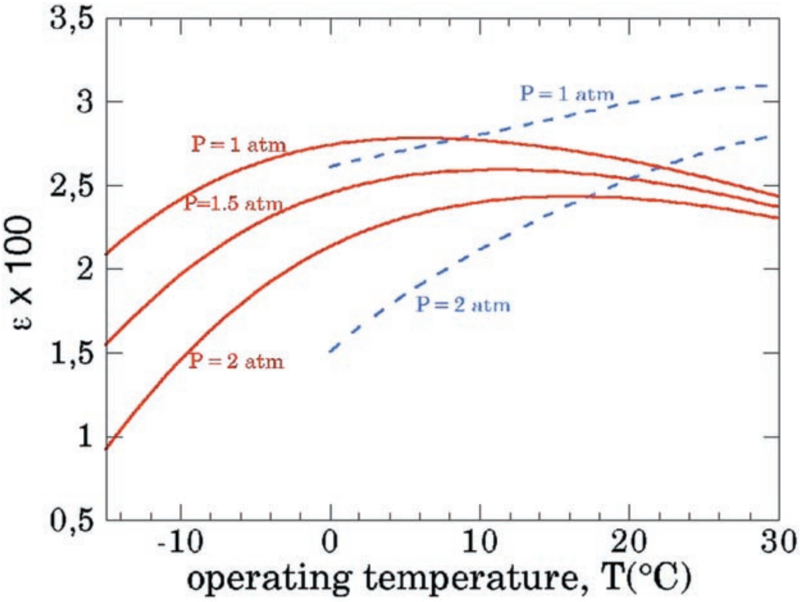

Figure 1. Calculated ϵ for R-115 (C_2ClF_5, solid red lines) and R-12 (CCl_2F_2, dashed blue lines) as a function of P and T.

The second condition in equation (1) can be exploited to avoid the background from ubiquitous minimally ionizing radiation that plagues experiments aiming to detect WIMP-induced nuclear recoils (WIMPs are one of the best candidates for the galactic dark matter [7]). SDDs of active mass $O(1)$ kg can in principle considerably extend the present experimental sensitivity [8] well into the region where new supersymmetric particles are expected. The low interaction rate expected from these particles (< 10 recoils kg^{-1} target mass day^{-1}) and the modest active mass of commercially available SDDs ($\simeq$0.03 g refrigerant per dosimeter), together with a desire to control and understand the fabrication process, led us to develop in collaboration with COMEX-PRO [9] a large-volume (80 l) pressure reactor dedicated to SDD production. Able to withstand 60 atm, it houses a variable-speed magnetic stirrer, heating and cooling elements and micropumps for the addition of catalysts whenever chemical cross linking of the gel is required. We have nevertheless favoured thermally reversible food gels such as agarose, gelatine and κ-carrageenan, due to concerns regarding safety in the handling of large volumes of synthetic monomers. The fabrication of 1 l SDD modules containing up to 3% of the superheated liquid starts with the preparation of a suitable gel matrix; the constituent materials must be carefully selected and processed in order to avoid the presence of alpha emitters, the only internal radioactive contaminants of concern [8]. A still with all contacting parts made of quartz and Teflon is used to produce high-purity bidistilled water. Unfortunately, a very precise density matching between the matrix and refrigerant is needed in order to obtain a uniform droplet dispersion, making water-based gels inadequate unless large fractions of inorganic salts are added, which can unbalance the chemistry of the composite and contribute an undesirable concentration of alpha emitters [10]. We find that glycerol is for this and other reasons an additive of choice. The gelating agent, polymer additives and glycerol are purified using a pre-eluted ion-exchanging resin specifically targeted at actinide removal. All components are forced through $0.2\ \mu$m filters to remove motes that might act as nucleation centres. The resulting mixture is

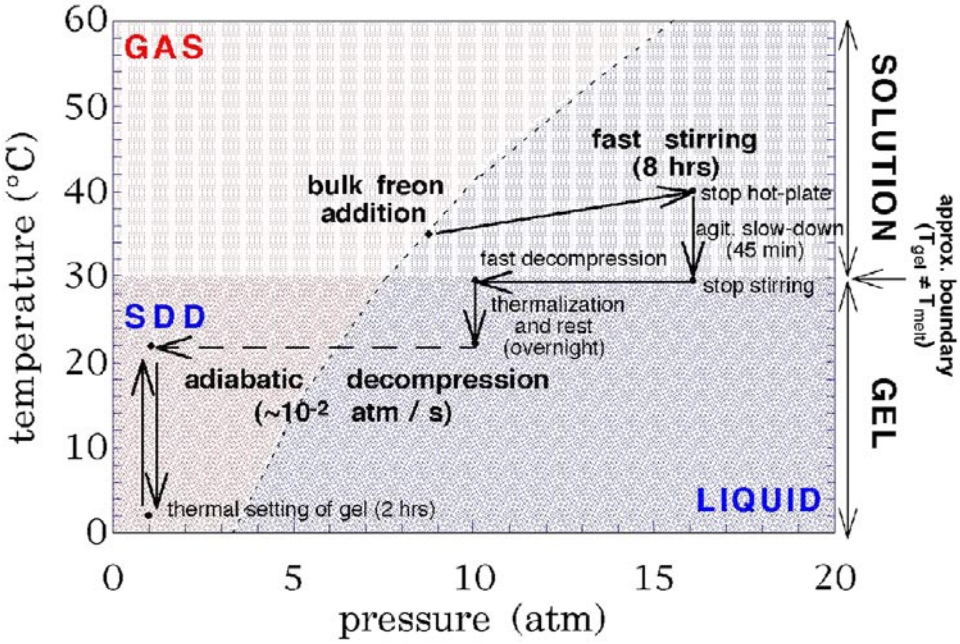

Figure 2. A schematic representation of the fabrication of a R-12 SDD. The blue region denotes the liquid phase of the refrigerant; pink is for gas. Their boundary (dotted line) traces $T(P_V)$. As a result of the adiabatic crossing of $T(P_V)$, the refrigerant remains in the (superheated) liquid state. The horizontal division between the sol and gel states of the matrix is only approximate, since the melting and gelation temperatures are not the same. The fabrication path changes radically for other refrigerants.

outgassed and maintained above its gelation temperature in the reactor. The refrigerant is distilled once prior to its incorporation into this solution, which is done at a pressure well above $P_V(T)$ to avoid boiling during the vigorous stirring that follows (figure 2). After a uniform dispersion of droplets has been obtained, cooling, setting and stepwise adiabatic decompression produce the delicate entanglement of superheated liquid and thermally reversible gel that makes up the SDD. Numerous practical precautions, to be described elsewhere, are necessary for producing stable modules; for instance, the stepwise decompression procedure used is identical to that employed by scuba divers returning to the surface, in order to minimize the cavitation of dissolved gas bubbles which, in SDDs, can act as inhomogeneous nucleation centres. The detectors are refrigerated and pressurized under 4 atm during storage and transportation, to inhibit their responses to environmental neutrons.

While SDDs can bypass the mentioned problems associated with a former [11] bubble chamber WIMP search proposal, they are not devoid of their own idiosyncrasies. During the R&D leading to the first SIMPLE modules, we have been able to identify and solve problems arising from some of the particularities of SDDs that can interfere with a successful WIMP search, for instance, the appearance of fractures in the gel and depletion of the active mass during long exposures via permeation processes. Another example is the formation of clathrate hydrates at the droplet boundaries during fabrication or recompression (these crystalline structures are able to destroy the metastability of the droplets). These detector improvements have been treated

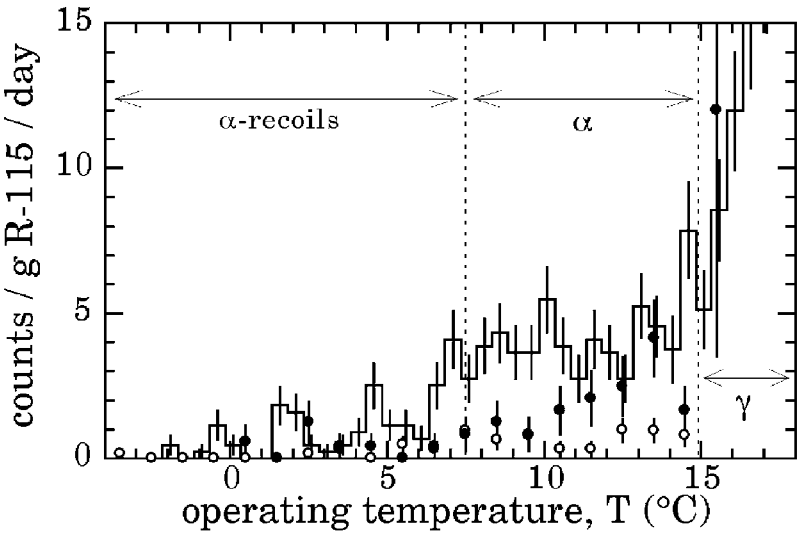

Figure 3. The SDD background at 90 m.w.e. and $P = 2$ atm, following cumulative steps of cleansing: histogram; double distillation of water and microfiltration; (•), single distillation of refrigerant and purification of glycerine; and (○), purification of gelatine and PVP. Vertical lines separate three different regimes of background dominance (see the text).

at some length elsewhere [12] and are summarized here in table 1. The objective was to keep the number of detector components to a minimum for reasons of radiopurity, safety and cost, while solving the condensed-matter issues as they appeared. Worthy of special mention are the gains in detector stability brought about by the transition from R-12 (CCl_2F_2) to R-115 (C_2ClF_5) (see table 1). Present SIMPLE modules contain $\simeq$1000 times the active mass of commercially available SDDs (limited only by the size of the pressure reactor) and can be operated continuously for up to $\simeq$40 days. Even though a further extension of this shelf life is intended, the design of recompression chambers that would allow an unlimited duration of exposure is being attempted. The cost of the SDD matrix has been kept down, allowing a much larger design in the future.

Prototype modules have been tested in an underground gallery 40 km south of Paris. The 27 m rock overburden and $\simeq$30 cm paraffin shielding reduce the flux of cosmic and muon-induced fast neutrons, which are the main sources of nucleations above ground. Inside the shielding, a water plus glycol thermally regulated bath maintains T constant to within $0.1\,°$C. The characteristic violent sound emission accompanying vaporization in superheated liquids [13, 14] is picked up by a small piezoelectric transducer in the interior of the module and then amplified and saved in a storage oscilloscope. Special precautions against acoustic and seismic noise are taken. Figure 3 displays the decrease in spontaneous bubble nucleation rate brought about by progressive purification of the modules that was measured at this site. The ability to rapidly modify the fabrication process and the choice of components has been critical in achieving this.

The response of smaller SDDs to various neutron fields has been studied extensively [6],[15, 16] and found to match theoretical expectations. However, large, opaque SDDs require independent calibration: acoustic detection of the explosion of the smallest or most distant droplets is not guaranteed *a priori*. The energy released as sound varies as $(P_V - P)^{3/2}$

Table 1. Characteristics of the present SIMPLE SDDs.

Component	Features	Goal
Water	Immiscible with most H-free refrigerants	Chemical compatibility
	Bidistilled (in a quartz and Teflon still)	Radiopurity
Glycerine	Density matching between sol and freon	Homogeneity of SDDs
	Viscosity enhancer	Fracture control (decreases diffusion)
	Solvent behaviour similar to that of water	Chemical compatibility
	Excellent wetting of glass surfaces	Absence of nucleations on walls
	Low U and Th content and easy to purify	Radiopurity
	Does not crystallize at low T	Lack of inhomogeneous nucleations
	Germicidal action at high percentage	No need to add preservatives
	Strengthens gelatine gels	Structural stability
PVP	Viscosity enhancer	Fracture control (decreases diffusion)
	Surfactant	Homogeneity of SDDs
	Salting-out agent at low percentage	Fracture control (decreases solubility)
	Kinetic inhibitor at low percentage	Absence of clathrate hydrates
	Compatible with gelatine gels	Chemical compatibility
	Chelating agent	Stops migration of alpha emitters to droplet boundaries
Gelatine	Forms a compliant gel in the relevant T range	Structural stability
	Non-toxic	Safety
	Low U and Th content (depends on organ origin)	Radiopurity
R-115	62% F (twice as much as R-12)	Higher sensitivity to WIMPs
(C_2ClF_5)	Non-toxic, non-flammable	Safety
	Much lower solubility than that of R-12	Control of fractures and active-mass losses
	Much larger molecule than R-12	Clathrates impossible, decreases diffusion
	Higher P_V than that of R-12, so it allows operation at lower T	Fracture control, decreases diffusion
	Operation at 2 atm	Fracture control and keeps radon out

[14], making these additional characterizations even more imperative for SDDs operated under moderate P. Two separate types of calibration have been performed to determine the target mass effectively monitored in SIMPLE modules and to check the calculation of the T, P-dependent threshold energy E_{thr} above which WIMP recoils can induce nucleations (defined as the lowest energy satisfying both conditions in equation (1) [8, 17]). First, a liquid $^{241}\mathrm{Am}$ source (an alpha emitter) is uniformly diluted into the matrix prior to gel setting. According to equation (1), the 5.5 MeV alpha particles and 91 keV recoiling $^{237}\mathrm{Np}$ daughters cannot induce nucleations at

temperatures below T_α and $T_{\alpha r}$, respectively [8]. The expression $a = 4.3(\rho_v/\rho_l)^{1/3}$ [6], where $\rho_l(T)$ is the saturated liquid density of the refrigerant, correctly predicts the observed T_α both for R-12 and for R-115 at $P = 1$ and 2 atm. Under similar conditions, the theoretical value of ϵ for these liquids (figure 1) accurately predicts the experimental $T_{\alpha r}$ (figure 4), which directly depends on it. Calibrations like those in figure 4 allow one to corroborate the calculation of E_c for each refrigerant: a good knowledge of E_c is crucial to determine the expected sensitivity of SDDs to WIMP recoils at various operating P and T.

Prior to extensive component purification, the spectrum in non-calibration runs (figure 3, histogram) had a close resemblance to that produced by $^{241}\mathrm{Am}$ spiking; the initial presence of a small ($\simeq 10^{-4}$ pCi g^{-1}) $^{228}\mathrm{Th}$ contamination, compatible with the observed rate, was confirmed via low-level alpha spectroscopy. Three regimes of background dominance are therefore delimited by vertical lines in figure 3: the sudden rise at $T \simeq 15\,^\circ$C originates from high-$\mathrm{d}E/\mathrm{d}x$ Auger electron cascades following interactions of environmental gamma rays with Cl atoms in the refrigerant [4, 18, 19]. The calculated E_c for R-115 at $T = 15.5\,^\circ$C and $P = 2$ atm is 2.9 keV, which coincides with the binding energy of K-shell electrons in Cl, 2.8 keV (i.e. the maximum E deposited via this mechanism). Thus, the onset of gamma sensitivity provides an additional check of the threshold in the few-kilo-electron-volt region.

Alpha calibrations cannot be used for a rigorous determination of the overall sound detection efficiency because a large fraction of the added emitters drifts to gel–droplet boundaries during fabrication, an effect explained by the polarity of actinide complex ions [20]. We observe that this effect is seemingly dependent on the matrix composition (the migration can be controlled to some extent by the addition of chelating polymers such as PVP, which can link to the actinides while becoming themselves immobilized by entanglement in the gel structure). Although this migration does not alter the expected values of T_α and $T_{\alpha r}$, it enhances the overall nucleation efficiency in a somewhat unpredictable manner [20]. To complete our understanding of the detector efficiency, SIMPLE modules have been exposed to a well-characterized $^{252}\mathrm{Cf}$ neutron source at the TIS/RP calibration facility (CERN). The resulting spectrum of neutron-induced fluorine recoils (figure 5, insert) mimics a typically expected one from WIMP interactions. A complete MCNP4a [21] simulation of the calibration set-up takes into account the small contributions from albedo and thermal neutrons. The expected nucleation rate as a function of T is calculated as in [8, 15]: cross sections for the elastic, inelastic, (n,α) and (n,p) channels of the refrigerant constituents are extracted from ENDFB-VI libraries. Look-up tables of the distribution of deposited energies as a function of the neutron energy are built from the SPECTER code [22] and stopping powers of the recoiling species are taken from SRIM98 [23]. Since T was continuously ramped up during the irradiations at a relatively fast $1.1\,^\circ\mathrm{C\ h}^{-1}$, a small correction to it (<1 °C) is numerically computed and applied to account for the slow thermalization of the module. Depending on T, the value of E_{thr} for elastic recoils of fluorine (the dominant nucleation mechanism in R-115) is set by either condition in equation (1), the other being always fulfilled for $E > E_{thr}$ [8, 17]. The handover from the second to the first condition at T above $\simeq 5.5\,^\circ$C ($\simeq 2.5\,^\circ$C) for $P = 2$ atm ($P = 1$ atm) is clearly observed in the data as two different regimes of the nucleation rate (figure 5).

A larger-than-expected response, already noticed in R-12 [6], is evident at low T: the calculated E_{thr} there is too conservative (too high). This behaviour appears well below the normal regime of SDD operation (which is at T high enough to have $E_{thr} = E_c$) and therefore does not interfere with neutron and WIMP detection. However, it is interesting in that it suggests that a higher than normal bubble nucleation efficiency can be obtained with heavy particles, as

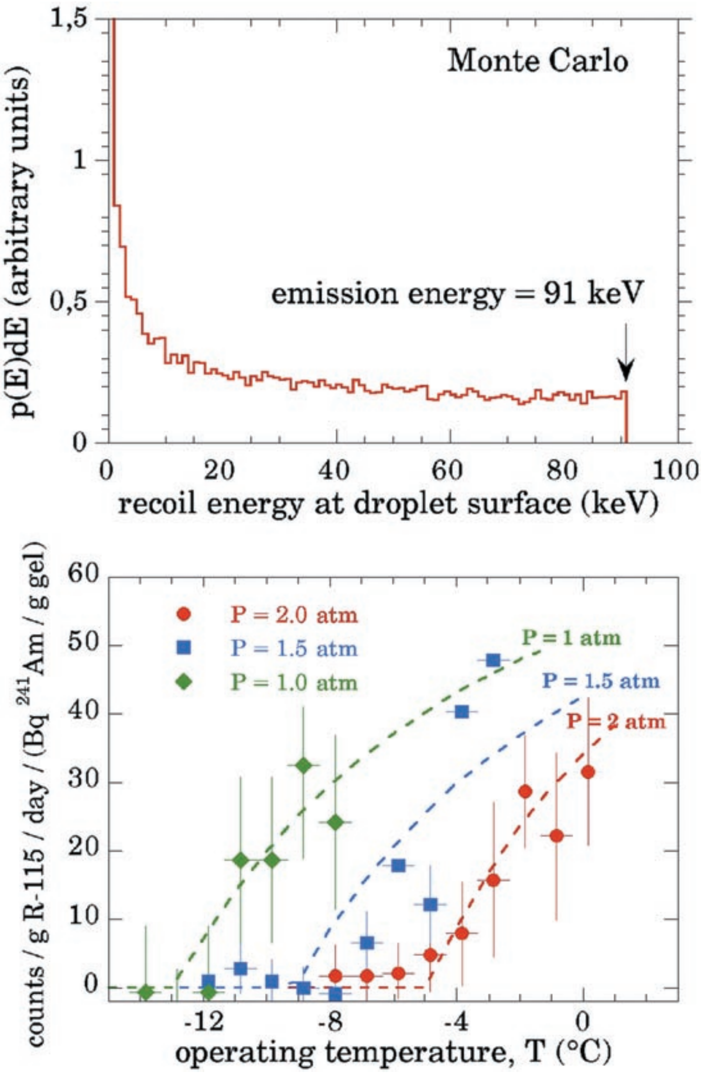

Figure 4. High-dE/dx recoiling Np daughters (emitted simultaneously with alpha decay of ^{241}Am in the gel) suffer energy losses prior to their arrival at a neighbouring droplet, resulting in a moderated energy spectrum (a) that falls in the same regime as that in which WIMP recoils are expected (a few tens of kilo-electron-volts). These recoils provide an opportunity to check the calculation of the minimum energy required for bubble formation (E_c, equations (1)–(3)): experimentally (b), the operating temperature $T_{\alpha r}$ above which they are able to produce nucleations is seen to vary with P following closely the theoretical predictions (dashed lines).

was discussed in early bubble chamber work [19]. It is precisely at low T that the spontaneous nucleation rate under low-background conditions is the smallest. Therefore this effect, which could greatly improve SDD WIMP limits, merits further attention: calibrations using filtered neutron beams of energies 2 ± 0.8, 24.3 ± 2, 55 ± 2 and 144 ± 24 keV available at the research reactor of the Nuclear and Technology Institute (Sacavem, Portugal) are planned as part of the SIMPLE 2000 effort. A best fit to the overall normalization of the Monte Carlo simulation over

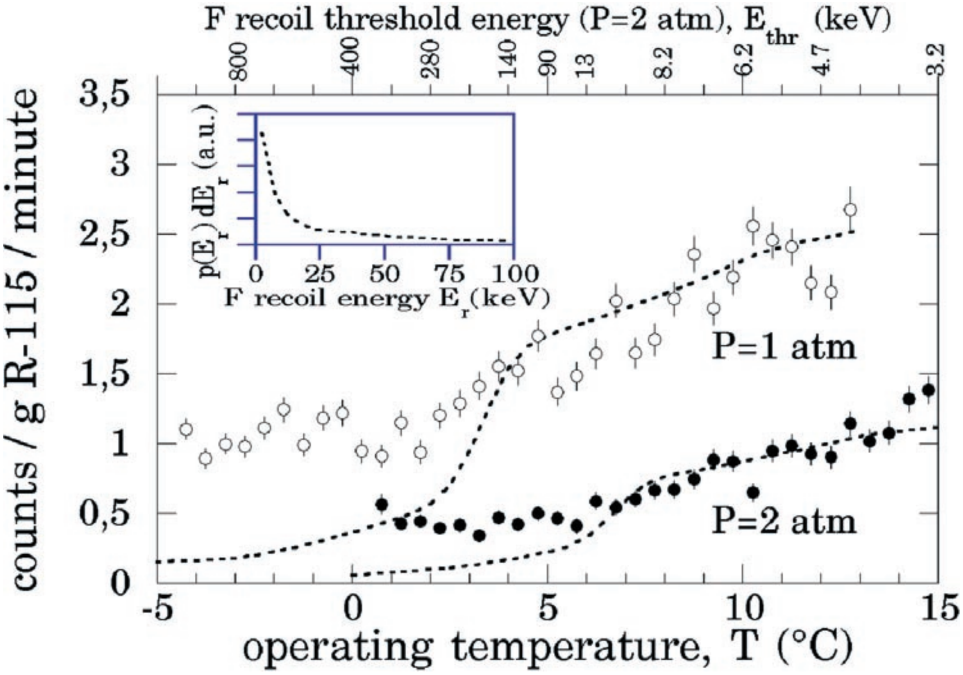

Figure 5. ^{252}Cf neutron calibration of SIMPLE modules at the TIS/RP bench (CERN), compared with Monte Carlo expectations (dotted lines, see text). The signal-to-noise ratio was >30 at all times. The inset shows the calculated energy spectrum of F recoils during the irradiations.

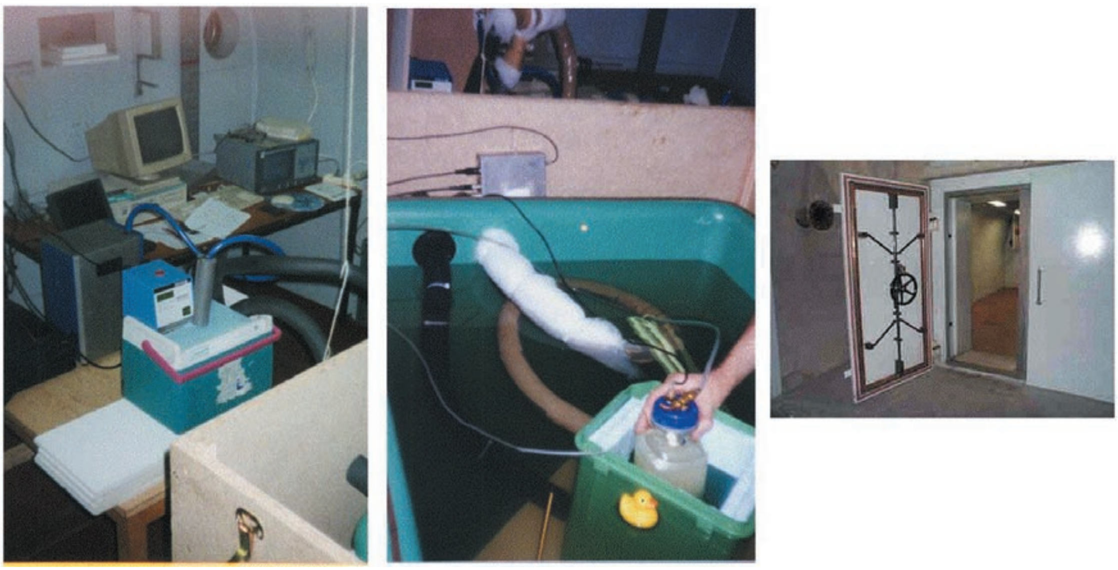

Figure 6. SIMPLE at 1500 m.w.e.. The left-hand picture shows the DAQ system and water temperature controlling system. The middle picture shows the first 9.2 g R-115 module being immersed in the 700 l of water used as a neutron moderator; sound and T insulating layers of the shielding are apparent. The right-hand picture shows the entrance to the experimental hall. The Cu–Be contacts that close the Faraday cage are visible on the rim of the door.

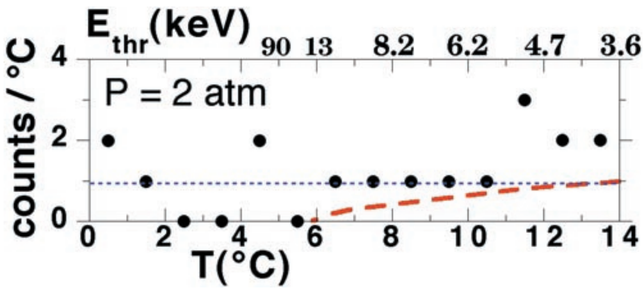

Figure 7. The counting rate in the first SIMPLE module installed in Rustrel (9.2 ± 0.1 g R-115, $\Delta T = -0.75\,°\mathrm{C\ day}^{-1}$). The top axis displays the calculated threshold energy for bubble nucleation from fluorine recoils. The blue dotted line indicates the average level of spurious background observed in refrigerant-free runs (see the text). The red broken line is the expected signal (accounting for 34% sound detection efficiency and F fraction) from a WIMP of mass $m_\chi = 10$ GeV and $\sigma_{Wp} = 5$ pb, i.e. at the limit of sensitivity of the DAMA experiment; present SIMPLE limits are largely limited by poor statistics.

the full data set (figure 5) allows us to determine the refrigerant mass monitored with the present sound acquisition chain as $34 \pm 2\%$ ($74 \pm 4\%$) of the total at $P = 2$ atm ($P = 1$ atm), a decisive datum for obtaining dark matter limits.

The installation 500 m underground of modules identical in composition, preparation and sound detection system to those utilized in ^{252}Cf calibrations started in July 1999 (figure 6). A decommissioned nuclear missile launching control centre has been converted into an underground laboratory [24], facilitating this and other initiatives. The characteristics of this site (microphonic silence, unique electromagnetic shielding of the halls [24]) make it especially adequate for rare-event searches. Modules are placed inside a thermally regulated water bath, surrounded by three layers of sound and thermal insulation. A 700 l water pool acting as neutron moderator, resting on a dual vibration absorber, completes the shielding. Events in the modules and in external acoustic and seismic monitors are time tagged, allowing one to filter out the small percentage ($\simeq 15\%$) of signals correlated to human activity in the immediate vicinity of the experiment. The signal waveforms are digitally stored, but no event rejection on the basis of pulse-shape considerations [10] is performed at this stage, avoiding the criticisms [25] associated with some WIMP searches in which large cuts to the data are made. The raw counting rate from the first SIMPLE module operated under these conditions is shown in figure 7. Accounting for the sound detection efficiency and a 62% fluorine mass fraction in R-115, limits on the spin-dependent WIMP–proton cross section σ_{Wp} can be extracted (figure 8). The cosmological parameters and method described in [26] are used in the calculation of WIMP elastic scattering rates, which are then compared with the observed uncut nucleation rate at $10\,°$C ($14\,°$C for small WIMP masses). The expected nucleation rate at T (i.e. the rate integrated over recoil energies above $E_{thr}(T)$) from a candidate at the edge of the sensitivity of the leading DAMA experiment [27] ($\simeq 1.5 \times 10^4$ kg day of NaI) is offered as a reference in figure 7: evidently, with the same level of background but significantly smaller statistical error bars, this candidate could have been marginally excluded. The present SIMPLE limits are impaired by the large statistical uncertainty associated with the short exposure accumulated so far, not yet by the background rate. A considerable improvement is expected after the ongoing expansion of the bath to accommodate up to 16 modules (figure 8).

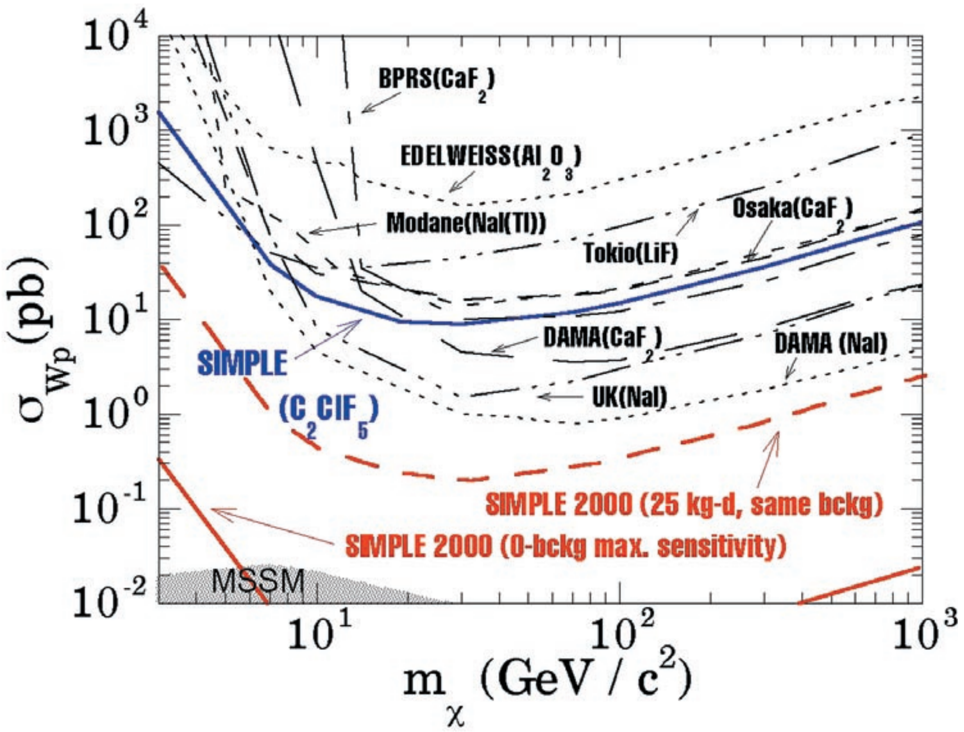

Figure 8. 95% C.L. limits on σ_{Wp} extracted from only 0.19 kg day of SDD exposure, compared with other experiments [26]. The red lines indicate the expected sensitivity of SIMPLE 2000 after an exposure of 25 kg day, if no improvement in the background is obtained (broken line) or at the maximum level attainable for this exposure (zero background, full red line off the scale). MSSM marks the tip of the region where a lightest supersymmetric partner is expected.

SIMPLE 2000 aims at an exposure of $\simeq$25 kg day in the next few months, by replacing the detectors (in batches of eight) every four to six weeks, repeating this cycle several times. A weak Am/Be neutron source will be used at the end of each run to assess the sound detection efficiency for each module *in situ*. In parallel to this, plastic module caps are being replaced by a sturdier design: runs using refrigerant-free modules show that *a majority* of the prototype events arose from pressure microleaks, correlated to the sense of T ramping, able to stimulate the piezoelectric sensor (figures 7 and 9). In principle, if this source of background is controlled, the maximum sensitivity of SIMPLE 2000 can start to probe the spin-dependent neutralino parameter space (figure 8). It must also be borne in mind that a T-independent, flat background implies a null WIMP signal, albeit this possible approach to data analysis can be exploited only after a sizable reduction in statistical uncertainty has been achieved.

The importance of the spin-dependent WIMP interaction channel, for which fluorine-rich detectors are by far the optimal target [28], has recently been emphasized by its relative insensitivity to *CP*-violation parameter values, which may otherwise severely reduce coherent (i.e. spin-independent) interaction rates [29]. To further stress the significance of this channel, we illustrate in figure 10 a not-so-obvious complementarity of spin-dependent and spin-independent searches in exploring the neutralino phase space. The top-left-hand frame displays points

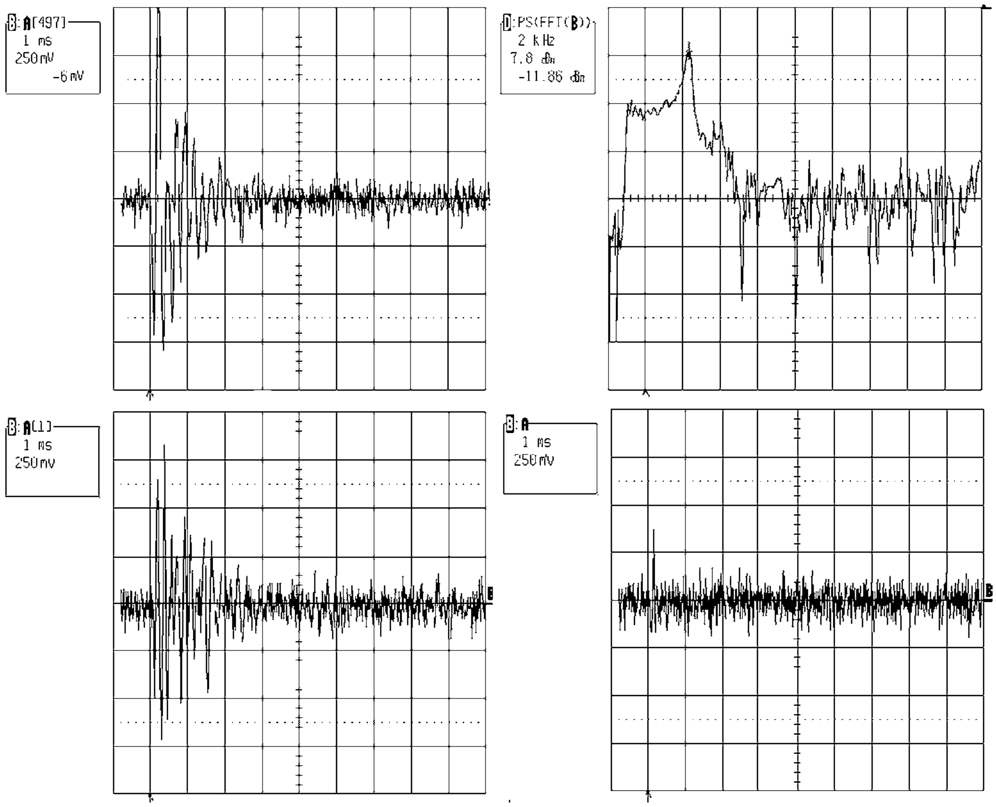

Figure 9. Signal and noise in present SIMPLE modules: the pulse shape (top-left-hand plot) corresponds to a typical bubble nucleation, with a dominant frequency of $\simeq$5 kHz (the top-right-hand plot shows its Fourier transform) and a time span of a few millisecond. During runs with refrigerant-free 'dummy' modules, similar signals (bottom-left-hand plot) arising from pressure microleaks in plastic SDD caps are observed at a rate of $\simeq 1\ \mathrm{day}^{-1}$. Even at atmospheric pressure, a residual rate of $\simeq 0.3\ \mathrm{day}^{-1}$ of characteristic EM noise events (bottom-right-hand plot) is present. As a first measure to deal with this, sturdier metallic SDD caps have been built and all inessential equipment (the PC and water chiller) is to be moved outside the Faraday cage. The sharply resonant piezoelectric sensors employed at present will eventually be replaced by others with a flatter spectral response, allowing unequivocal identification of the nucleation sounds.

generated with the help of the NEUTDRIVER code [7], each representing a possible combination of MSSM parameters. The parameter space sampled is the same as that in [30] (namely, $10\,\mathrm{GeV} \leq M_2 \leq 10\,\mathrm{TeV}, 10\,\mathrm{GeV} \leq \mid \mu \mid \leq 10\,\mathrm{TeV}, 1.1 \leq \tan(\beta) \leq 50, 60\,\mathrm{GeV} \leq m_A \leq 1\,\mathrm{TeV}$ and $100\ \mathrm{GeV} \leq m_0 \leq 1\ \mathrm{TeV}$) and special precautions are taken to do so as homogeneously as possible, within the limitations imposed by computing time. Only a weak correlation between the values of σ_{Wp} (i.e. the spin-dependent coupling strength, corrected for the local halo density) and σ_{Wn} (spin-independent) is observed in the plot (note the scale). As a result of this, a compact ($\simeq$1 kg active mass), low-background SDD starting to probe the neutralino σ_{Wp} (top-right-hand frame) generates a rather homogeneous 'cleaning' of the MSSM models in a σ_{Wn} exclusion plot (bottom-left-hand frame, without the constraints imposed by the limits in the top-right-hand

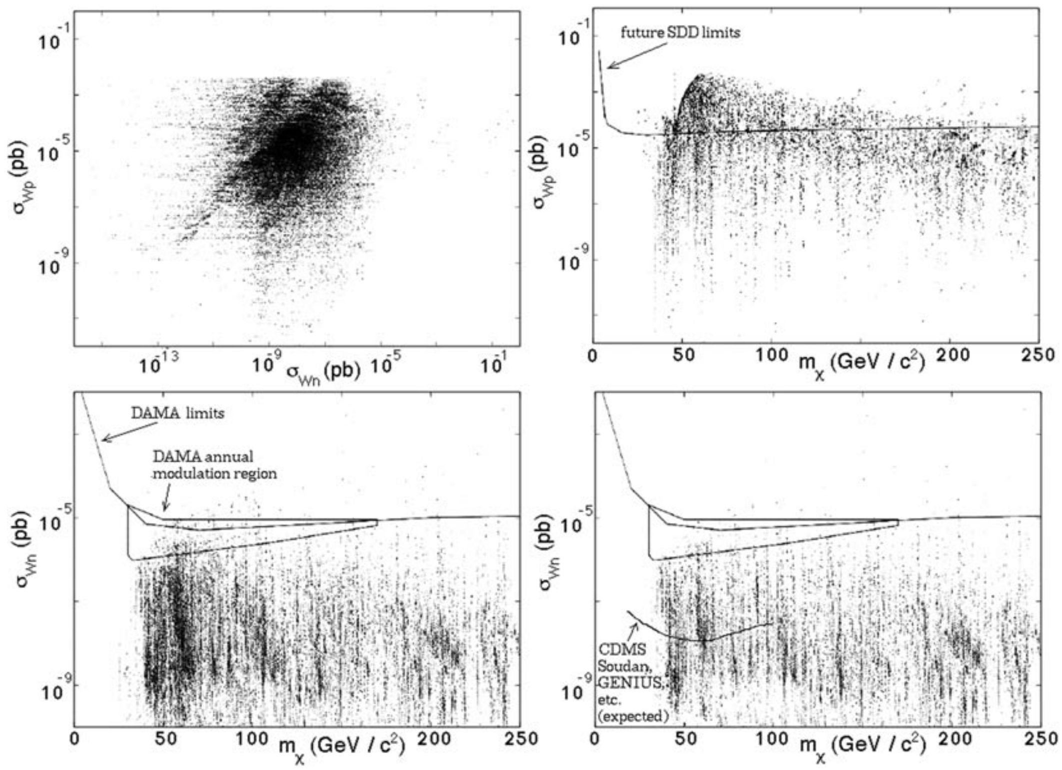

Figure 10. A fluorine-rich SDD of modest active mass ($O(1)$ kg), the ultimate goal of the SIMPLE programme, will be sensitive to neutralino WIMP candidates beyond the reach of the most ambitious planned cryogenic experiments (see the text).

frame; with them in the bottom-right-hand frame), down to values of σ_{Wn} far beyond the reach of the most ambitious planned cryogenic WIMP searches. This can be counter-intuitive for the hardcore experimentalist, who might otherwise naively expect the SDD to take only a small bite off the top of the σ_{Wn} cloud in the lower-left-hand frame (in other words, might expect much more of a correlation between σ_{Wp} and σ_{Wn}). Needless to say, the converse can be stated of the way that cutting-edge spin-independent searches will deplete the σ_{Wp} cloud and hence the complementarity of these two approaches. In conclusion, if an exhaustive test of the neutralino-as-cold-dark-matter hypothesis is ever to be achieved, the development of fluorine-rich detectors cannot be neglected: in this respect SDDs represent an ideal opportunity.

Acknowledgments

We thank the Communauté des Communes du Pays d'Apt and French Ministry of Defence for supporting the conversion of the underground site. G Jungman graciously provided the NEUTDRIVER code and assistance with implementing it. Our gratitude also goes to M Auguste, J Bourges, G Boyer, R Brodzinski, A Cavaillou, COMEX-PRO, M El-Majd, M Embid, L Ibtiouene, IMEC, J Matricon, M Minowa, Y H Mori, T Otto, G Roubaud, M Same and C W Thomas. JIC was supported by the TMR programme of the EU.

References

[1] Apfel R E 1979 *Nucl. Instrum. Methods* **162** 603
[2] Seitz F 1958 *Phys. Fluids* **1** 1
[3] Roy S C *et al* 1987 *Nucl. Instrum. Methods* A **255** 199
[4] Peyrou Ch 1967 *Bubble and Spark Chambers* ed R P Shutt (New York: Academic)
[5] Apfel R E *et al* 1985 *Phys. Rev.* A **31** 3194
[6] Harper M 1991 *PhD Dissertation* (University of Maryland)
Harper M 1993 *Nucl. Sci. Engng* **114** 118
Harper M 1993 *Nucl. Instrum. Methods* A **336** 220
[7] Jungman G *et al* 1996 *Phys. Rep.* **267** 195
[8] Collar J I 1996 *Phys. Rev.* D **54** R1247
[9] COMEX-PRO, 36 Boulevard des Océans, 13275 Marseille, France
[10] Hamel L A *et al* 1997 *Nucl. Instrum. Methods* A **388** 91
[11] Zacek V 1994 *Nuovo Cimento* A **107** 291
[12] Collar J I *et al* astro-ph/0001511 (submitted to *Phys. Rev. Lett.*)
Collar J I *et al* 1999 *Proc. Topics in Astroparticle and Underground Physics, (Paris, 1999)* to be published in *Nucl. Phys.* B (*Proc. Suppl.*), transparencies available from http://taup99.in2p3.fr/TAUP99/Monday/monday.html
Collar J I *et al* 1999 *Proc. VIIIth Int. Conf. on Calorimetry in High Energy Physics, (Lisbon, 1999)*
Collar J I *et al* 1999 *Proc. 2nd Int. Workshop on the Identification of Dark Matter, (Buxton, 1998)* (Singapore: World Scientific)
astro-ph/9610266, 1997 *Proc. 1st Int. Workshop on the Identification of Dark Matter, (Sheffield, 1996)* (Singapore: World Scientific)
[13] Apfel R E *et al* 1983 *Rev. Sci. Instrum.* **54** 1397
[14] Martynyuk Yu N and Smirnova N S 1991 *Sov. Phys.–Acoust.* **37** 376
Aleksandrov Yu A *et al* 1967 *Bubble Chambers* (Bloomington: Indiana University Press) p 29
[15] Lo Y-Ch and Apfel R 1988 *Phys. Rev.* A **38** 5260
[16] d'Errico F 1999 *Radiat. Prot. Dosimetry* **84** 55
[17] El-Nagdy M *et al* 1971 *J. Br. Nucl. Engng Soc.* **10** 131
[18] Riepe G and Hahn B 1961 *Helv. Phys. Acta* **34** 865
[19] Tenner A G 1963 *Nucl. Instrum. Methods* **22** 1
[20] Pan L K *et al* 1999 *Nucl. Instrum. Methods* A **420** 345
[21] Briesmeister J F (ed) 1993 *MCNP, A General Monte Carlo* N-*Particle Transport Code* (Los Alamos: Los Alamos National Laboratory)
[22] Greenwood L R and Smither R K 1985 *SPECTER, Neutron Damage Calculations for Materials Irradiations* (Argonne National Laboratory)
[23] http://www.research.ibm.com/ionbeams/
[24] http://home.cern.ch/collar/RUSTREL/rustrel.html, http://iapetus.unice.fr/∼rustreou/
Waysand G *et al* astro-ph/9910192
[25] Gerbier G *et al* 1999 *Astropart. Phys.* **11** 287
[26] Smith P F *et al* 1996 *Phys. Lett.* B **379** 299
Lewin J D and Smith P F 1996 *Astropart. Phys.* **6** 87
[27] See relevant contributions in 1999 *Proc. 2nd Int. Workshop on the Identification of Dark Matter, (Buxton, 1998)* (Singapore: World Scientific)
[28] Ellis J and Flores R A 1991 *Phys. Lett.* B **263** 259
[29] Falk T *et al* hep-ph/9806413
Gondolo P and Nath P, private communication
[30] Bottino A astro-ph/9611137